J Mater Sci (2009) 44:2792–2795
DOI 10.1007/s10853-009-3367-1

Synthesis and luminescence properties of ZnS:Mn/ZnS core/shell nanorod structures

Daixun Jiang · Lixin Cao · Ge Su · Wei Liu · Hua Qu · Yuanguang Sun · Bohua Dong

Received: 21 November 2008 / Accepted: 23 February 2009 / Published online: 19 March 2009

Abstract Mn-doped ZnS nanorods synthesized by solvothermal method were successfully coated with ZnS shells of various thicknesses. The powder X-ray diffraction (XRD) measurements showed the ZnS:Mn nanorods were wurtzite structure with preferential orientation along c-axis. Transmission electron microscopy images (TEM) revealed that the ZnS shells formed from small particles, growing along a-axis orientation, which was proved by the XRD measurements. Room temperature photoluminescence (PL) spectra showed that the intensity of Mn emission first increased and then decreased with the thickening of the ZnS shells. The effects of ZnS shells on the luminescence properties of ZnS:Mn nanorods is discussed.

Introduction

Nanoscale semiconductor materials doped with impurities as activators have been the subject of an extensive research interest in recent years due to their applications for a variety of commercial devices [1–5]. The doping ions act as recombination centers for the excited electron-hole pairs and play an influential role in determining optical properties, resulting in strong and characteristic luminescence. As one of well-known II–VI compound semiconductors, ZnS is particularly suitable for use as luminescent host materials for a variety of dopants due to its wide band gap energy at room temperature. One can easily achieve photoluminescence (PL) at different wavelengths by doping ZnS with different activating metal ions [6–10]. Among them, Mn-doped ZnS nanocrystals have been given much more research attention, mainly because of their promising applications. Unfortunately, a large portion of atoms are located on or near surfaces because of their high surface-to-volume ratio arising from the small particle size. This causes the surface states to act as luminescent quenching centers, resulting in low luminescence efficiency. In order to conquer such serious shortcomings, accordingly, core/shell structural nanomaterials have been developed and shown dramatically enhanced properties. Enhanced luminescence has been observed in ZnS:Mn/SiO_2 nanoparticles [11], ZnS:Mn/ZnS nanocrystals [12], ZnS:Mn/ZnO nanoparticles [13], and ZnS:Mn/$Zn(OH)_2$ nanocrystals [14].

As mentioned above, a great deal of effort has been devoted to the spherical core/shell structural nanocrystals, and researches on one-dimensional nanostructures, such as nanorods, nanotubes, nanowires, are infrequent. The PL properties of nanorods differ significantly from those of spherical nanocrystals. Compared with spherical nanocrystals, nanorods feature higher PL quantum efficiency, highly polarized PL, and significantly faster carrier relaxation [15]. One-dimensional nanostructures have also become the focus of intensive research owing to their unique applications in fabrication of nanoscale devices [16].

In this article a convenient route to fabricate core/shell structural ZnS:Mn/ZnS nanorods is reported, and the impact of ZnS shells on the luminescence properties of Mn-doped ZnS nanorods is well studied.

Experimental details

Sample preparation

All the reactants and solvents used in this work were of analytical grade and used without any further purification.

D. Jiang · L. Cao (✉) · G. Su · W. Liu · H. Qu · Y. Sun · B. Dong
Institute of Materials Science and Engineering, Ocean University of China, Qingdao 266100, People's Republic of China
e-mail: caolixin@mail.ouc.edu.cn

In a typical synthesis process, 0.01 mol zinc acetate [$Zn(CH_3COO)_2 \cdot 2H_2O$], 0.01 mol thioacetamide [CH_3CSNH_2] and 5×10^{-5} mol manganese acetate [$Mn(CH_3COO)_2 \cdot 4H_2O$] were put into a Teflon-lined stainless steel autoclave of 72 mL capacity, and then the autoclave was filled with a mixture solvent of ethylenediamine and deionized water (in 1:1 volume ratio) to 80% of its total volume. After being sealed, the autoclave was maintained at 200 °C for 6 h and then cooled down to room temperature naturally. The final precipitates were separated by centrifugation at 5,000 rpm and washed with deionized water and absolute ethanol three times, respectively, to remove excessive ethylenediamine and by-products. The samples were then dried in vacuum at 50 °C for 5 h and collected for further characterization and treatment.

In order to make ZnS shells on the surface of ZnS:Mn nanorods, the precipitation reaction of $Zn(NO_3)_2$ and Na_2S was employed. Typically, 0.2 g previously prepared bare ZnS:Mn nanorods powder was put into 200-mL deionized water and ultrasonically dispersed for 1 h,followed by slow dropping of appropriate amount of 0.02 M $Zn(NO_3)_2$ aqueous solution into the ZnS:Mn nanorods suspension under vigorous stirring. 10 min later, after the drop process of $Zn(NO_3)_2$ aqueous solution, appropriate amount of 0.02 M Na_2S aqueous solution was very slowly dropped into the suspension to form stoichiometric ZnS. The nucleation and growth of a separate ZnS particle were suppressed by the very slow addition of the S^{2-} aqueous solution. After 10 min of continuous stirring, the resulting precipitates were treated in the same procedure as that for ZnS:Mn nanorods. The thickness of ZnS shell was controlled by varying the dosages of $Zn(NO_3)_2$ and Na_2S, as indicated in Table 1.

Characterization

A D8 ADVANVCE X-Ray diffractometer was used to characterize the crystal structure of samples. The morphologies (TEM) of samples were observed on a Hitachi H-7000 transmission electron microscope. The room temperature PL spectra were achieved by a Flurolog-3p fluorescence spectrophotometer.

Table 1 Dosages of $Zn(NO_3)_2$ aqueous solution and Na_2S aqueous solution used in forming ZnS shells (In the parentheses, 0, 0.1, 0.2, 0.3, 0.4, 0.5, and 1 are set to be the mole ratios of Zn^{2+} ions in shells and cores.)

Samples	Volume of $Zn(NO_3)_2$ aqueous solution (mL)	Volume of Na_2S aqueous solution (mL)
ZnS:Mn/ZnS(0)	0	0
ZnS:Mn/ZnS(0.1)	10	10
ZnS:Mn/ZnS(0.2)	20	20
ZnS:Mn/ZnS(0.3)	30	30
ZnS:Mn/ZnS(0.4)	40	40
ZnS:Mn/ZnS(0.5)	50	50
ZnS:Mn/ZnS(1)	100	100

Results and discussion

Morphology and structure

Figure 1 shows TEM images of two single ZnS:Mn nanorods. It can be seen from Fig. 1a that the nanorod used as nucleation center for the growth of ZnS shell is 30–40 nm in diameter and ~300 nm in length. Its surface is smooth, and shape is regular. From Fig. 1b, it can be observed that the ZnS shells grow on the surface of the ZnS:Mn nanorods in the form of small particles.

Figure 2 shows some representative X-ray diffraction (XRD) patterns of ZnS:Mn nanorods without or with ZnS shells. In Fig. 2, all the diffraction peaks of the ZnS:Mn nanorods without (Fig. 2a) and with (Fig. 2b–e) ZnS shells can be indexed as (100), (002), (101), (102), (110), (103), (112), and (201) planes, which match well with the standard card (JPCSD No. 05-0492), revealing both of the core and shell possess the wurtzite phase of ZnS. The strong (002) diffraction peak of bare ZnS:Mn nanorods indicates that the preferential orientation of ZnS:Mn nanorods is along the c-axis. The most interesting observation from XRD spectra is that the diffraction peak from (100) planes becomes gradually stronger with respect to (002) with the shells thickening, which demonstrates that the ZnS shells on the surface of ZnS:Mn nanorods grew along the a-axis.

Photoluminescence properties

The room temperature photoluminescence emission (PL) and excitation (PLE) spectra are given in Figs. 3 and 4, respectively. In Fig. 3, the PL spectra of all samples present one emission band at ~580 nm, which differs from the observation of three emission bands in Mn-doped ZnS nanorods prepared by Chaudhuri et al. [17]. The distinction is presumably due to the highly crystalline quality of ZnS:Mn nanorods reported in this article, indicated by the rather weak defect-related luminescence at ~500 nm. The strong orange emission at ~580 nm is caused by the transition from $^4T_1$ (excited) to $^6A_1$ (ground) of Mn^{2+} ions [18], indicating that the Mn^{2+} ions have been successfully incorporated into the ZnS host lattice [19]. As the thickness of ZnS shell increases, the emission intensity has an increase followed by a steady decline, which attains its maximum at 0.1 ZnS shell thickness. Usually, for the uncoated ZnS:Mn nanorods, there are some non-radiative recombination routes, which are related to Mn^{2+} ions on

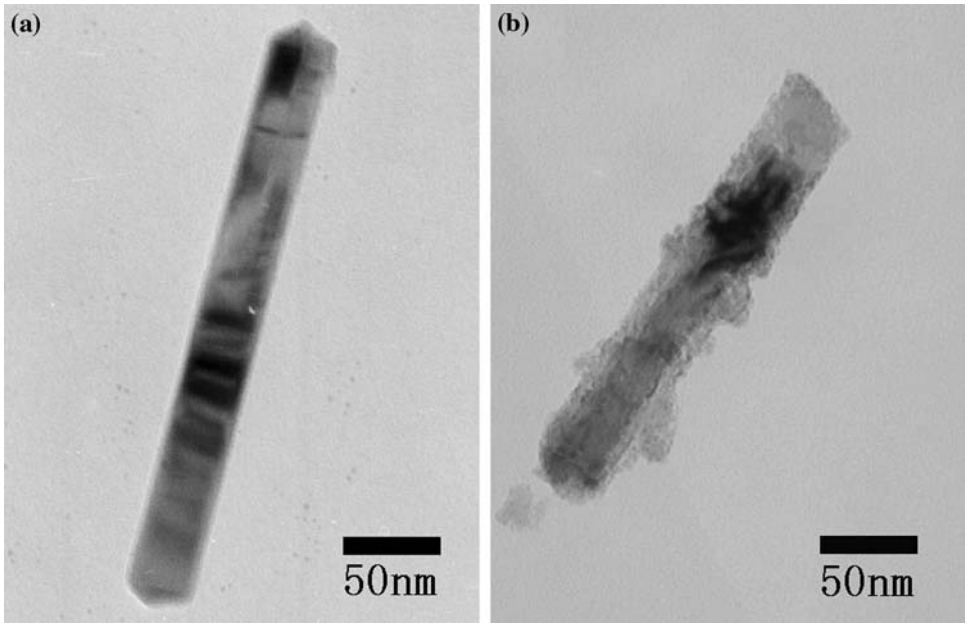

Fig. 1 TEM images of two ZnS:Mn nanorods **a** without and **b** with ZnS shell (a) ZnS:Mn/ZnS(0); (b) ZnS:Mn/ZnS(1)

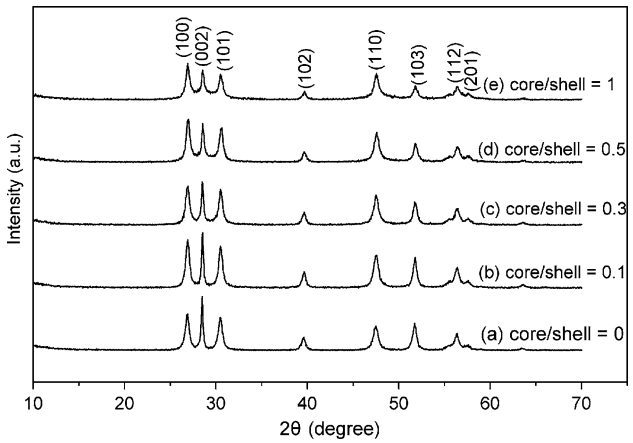

Fig. 2 XRD patterns of ZnS:Mn nanorods (a) without and (b, c, d, e) with ZnS shells of different thicknesses

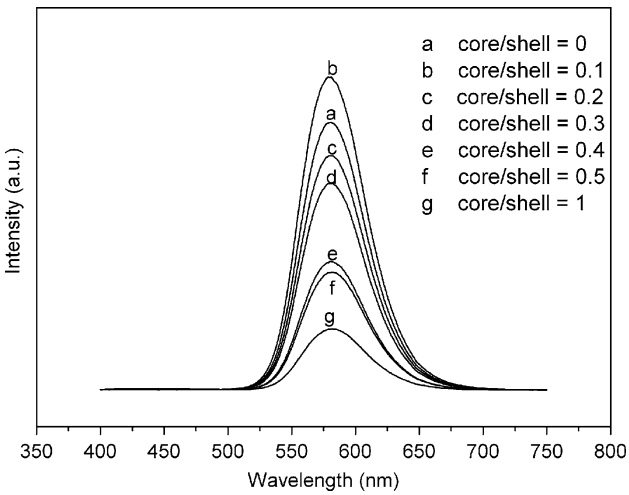

Fig. 3 Room temperature photoluminescence (PL) spectra of ZnS:Mn nanorods (a) without and (b–g) with ZnS shells of different thicknesses

the surface of the nanorods, giving rise to reduction in the PL intensity. When the surface of ZnS:Mn nanorods is coated by a thin ZnS shell, the number of the Mn^{2+} ions on the surface is reduced, resulting in blocking some non-radiative recombination routes. Hence, the PL intensity of Mn emission was enhanced through the increase of radiative transition of Mn^{2+} ions. However, the luminescence enhancement effect of ZnS shells will be weaker as shell thickening, because the Mn^{2+} ions on the surface of the nanorods have been annihilated progressively. On the other hand, the concentration of luminescent center (Mn^{2+} ions) was gradually reduced with increasing thickness of the shell, which would therefore decrease the intensity of Mn emission. Moreover, according to literature [20], the growth of ZnS shells may begin with a large density of nucleation sites producing many, small island-like ZnS clusters with a structure locally coherent with the core (ZnS:Mn nanorods). These islands then coalesce to form small ZnS particles, and the formation of grain boundaries could then be non-radiative recombination sites, which may also be a possible reason for the reduction in PL intensity. So the decreases of luminescent center concentration and the potential increase of non-radiative recombination sites will lead the steady reduction in PL intensity as shell thickening. As the ZnS shells have the two opposite effects on the luminescence properties of ZnS:Mn nanorods as discussed above, the intensity of Mn emission present the initial increase followed by the steady decline.

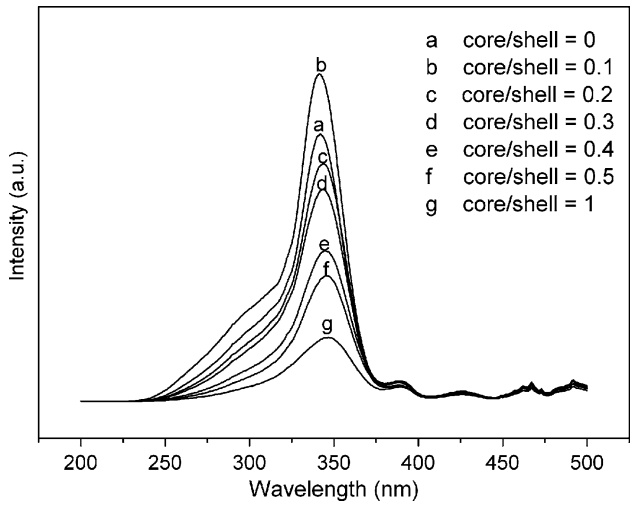

Fig. 4 Room temperature photoluminescence excitation (PLE) spectra of ZnS:Mn nanorods (a) without and (b–g) with ZnS shells of different thicknesses

The luminescence excitation in doped semiconductors can be accomplished by two channels, i.e., indirect excitation into the excited levels of the host, followed by energy transfer from the host to the impurity ions inducing the luminescence, and direct excitation of the impurity ions [21]. In Fig. 4, the excitation spectra monitoring the characteristic emission of Mn^{2+} ions show a leading broad band centering at $\sim$340 nm, which is the indirect excitation of ZnS host. There also exist four weaker spectral peaks at the long wavelength from 394 nm to 491 nm. These are direct excitation peaks of Mn^{2+} ions, whose centers are at 394 nm, 429 nm, 466 nm, and 491 nm, respectively. They should be attribute to intraconfigurational transitions of the $3d^5$ multiplet states of Mn^{2+} ions, corresponding to the $^6A_1(^6S)$–$^4E(^4D)$, $^6A_1(^6S)$–$^4T_2(^4D)$, $^6A_1(^6S)$–$^4A_1(^4G)$, $^4E(^4G)$, and $^6A_1(^6S)$–$^4T_2(^4G)$ in the order of decreasing energy [21, 22]. The contrast of the intensity between the leading peak and the other four weaker peaks is very prominent, demonstrating that the emission of transition from $^4T_1$ to $^6A_1$ of Mn^{2+} ions takes place predominantly via the energy transfer from the excited ZnS host lattice to Mn^{2+} ions.

Conclusion

To summarize, Mn-doped ZnS nanorods have successfully been coated with ZnS shells of different thicknesses. The influence of ZnS shell thickness on the luminescence properties of ZnS:Mn nanorods has been well studied. TEM images and XRD measurements give evidence that the ZnS shells grow on the surfaces of ZnS:Mn nanorods in the form of small particles, with preferential orientation along a-axis. The effects, i.e., blocking some non-radiative recombination routes related to Mn^{2+} ions on the surface of the nanorods,decreasing the concentration of luminescent center and increasing the non-radiative recombination sites concerned with grain boundaries, are concurrent in the ZnS shells, which result in an increase in Mn emission followed by a steady decline in the PL spectra.

Acknowledgements The authors thank the National Science Foundation of China (NSFC 50672089) and the Encouraging Foundation for the Scientific Research of the Excellent Young and Middle-aged Scientists in Shandong Province (2006BS04034) for financial support.

References

1. Karar N, Singh F, Mehta BR (2004) J Appl Phys 95:656
2. Cruz AB, Shen Q, Toyoda T (2005) Mater Sci Eng C 25:761
3. Ding Y, Wang XD, Wang ZL (2004) Chem Phys Lett 398:32
4. Tang W, Cameron DC (1996) Thin Solid Films 280:221
5. Bredol M, Merikhi J (1998) J Mater Sci 33:471. doi:10.1023/A:1004396519134
6. Ehlert O, Osvet A, Batentschuk M, Winnacker A, Nann T (2006) J Phys Chem B 110:23175
7. Sapra S, Prakash A, Ghangrekar A, Periasamy N, Sarma DD (2005) J Phys Chem B 109:1663
8. Kushida T, Kurita A, Watanabe M, Kanematsu Y, Hirata K, Okubo N, Kanemitsu Y (2000) J Lumin 87–89:466
9. Tiseanu C, Mehra RK, Kho R, Kumke M (2003) J Phys Chem B 107:12153
10. Chen W, Malm JO, Zwiller V, Huang Y, Liu S, Wallenberg R, Bovin JO, Samuelson L (2000) Phys Rev B 61:11021
11. Hattori Y, Isobe T, Takahashi H, Itoh S (2005) J Lumin 113:69
12. Cao LX, Zhang JH, Ren SL, Huang SH (2002) Appl Phys Lett 80:4300
13. Karar N, Chander H, Shivaprasad SM (2004) Appl Phys Lett 85:5058
14. Jiang DX, Cao LX, Su G, Qu H, Sun DK (2007) Appl Surf Sci 253:9330
15. Shabaev A, Efros AL (2004) Nano Lett 4:1821
16. Xia Y, Yang P, Sun Y, Wu Y, Mayers B, Gates B, Yin Y, Kim F, Yan H (2003) Adv Mater 15:353
17. Biswas S, Kar S, Chaudhuri S (2005) J Phys Chem B 109:17526
18. Zhang Y, Li YD (2004) J Phys Chem B 108:17805
19. Hu H, Zhang WH (2006) Opt Mater 28:536
20. Dabbousi BO, Rodriguez-Viejo J, Mikulec FV, Heine JR, Mattoussi H, Ober R, Jensen KF, Bawendi MG (1997) J Phys Chem B 101:9463
21. Chen W, Sammynaiken R, Huang Y (2000) J Appl Phys 88:5188
22. Peng WQ, Qu SC, Cong GW, Zhang XQ, Wang ZG (2005) J Cryst Growth 282:179